Int J Adv Manuf Technol (2016) 84:347–360
DOI 10.1007/s00170-015-7577-1

ORIGINAL ARTICLE

Efficient statistical analysis of geometric tolerances using unified error distribution and an analytical variation model

Guo Chongying[1] · **Liu Jianhua**[1] · **Jiang Ke**[1]

Received: 1 December 2014 / Accepted: 6 July 2015 / Published online: 5 August 2015

Abstract Inaccuracies in conventional tolerance characterization methods, which are based on worst-case and root-square-error methods, as well as inefficiencies in Monte Carlo computational methods of statistical tolerance analysis, require an accurate and efficient method of statistical analysis of geometric tolerances. Here, we describe a unified error distribution model for various types of geometric tolerance to obtain the distribution of the deviations in different directions. The displacement distributions of planes, straight lines, and points are analyzed based on distributions within tolerance zones. The distribution of the displacements of clearance fits is then determined according to the precedence of the assembly constraints. We consider the accumulated assembly variations and displacement distributions, and an analytical model is constructed to calculate the distribution of the deviations of the control points and the process capability index to validate the functional requirements. The efficiency of the method is shown by applying it to the assembly of a single-rod piston cylinder. The results are compared with other statistical methods of tolerance analysis. We find an improvement of approximately 20 % in tolerance analysis, and the process capability index of the assembly procedure was reduced by 10 %.

Keywords Statistical tolerance analysis · Deviation direction · Geometric tolerance · Chi distribution

✉ Liu Jianhua
jeffliu@bit.edu.cn

[1] School of Mechanical Engineering, Beijing Institute of Technology, Beijing, China 100081

1 Introduction and purpose

Tolerance analysis is important in verifying the assemblability of parts, as well as in the quality of the assembled product. Conventional methods of tolerance analysis include the worst-case (WC) method and the root-square-sum (RSS) method. The WC method requires full interchangeability, i.e., the accuracy of the final calculation is required to be within the scope of the functional assembly requirements, and the assembly success probability is 100 %. The WC method is excessively strict, and results in large manufacturing costs to guarantee that assembly requirements are met. By contrast, the RSS method requires tarsus interchangeability, and errors in parts are assumed to be independent normally distributed. Because the deviations from the design geometry are identical for each orthogonal direction, we can use the variance to calculate the assembly precision. To ensure that *most* of the products are within the scope of assembly requirements, the calculation process is less stringent; however, the RSS method is often so lenient that assembly requirements are poorly satisfied. Consequently, neither the WC method nor the RSS method is a good description of the accumulated assembly variations.

Although manufacturing errors are uncertain, the distribution thereof can be well described. To improve the accuracy of error characterization, it is necessary to carry out a statistical tolerance analysis to determine the frequency distribution of the characteristics of the measured tolerances [1, 2]. Efficiency is also required for optimization of tolerances to avoid substantial computational costs. In addition, different types of geometric tolerance are commonly used in the design of parts to control the form, direction or/and position. Compared with dimensional tolerances, geometric tolerances may restrict the displacement of features along several constraint directions. Therefore, a multi-dimensional analysis is

required, which should consider the interrelations among displacement constraints within the tolerance zones.

The purpose of this study was to carry out a statistical analysis of geometric tolerances. An analytical model is used to describe assembly precision based on distributions of deviations in multiple degrees of freedom (DOFs). Based on the relationships between geometric errors and the multi-DOF deviations, distributions thereof are constrained by the geometric tolerances and fitting gaps. These are analyzed comprehensively for planes, straight lines, and points. A covariance analysis is then carried out for the accumulated assembly variations, and the assembly precision and assembly capability index are computed efficiently.

2 Literature review

Here, we focus on the error distributions of tolerances, assemblability of parts, and distributions of the resulting error. Although dependent on the tolerance type, the distribution of tolerances is typically characterized by dimensional errors and geometric errors. Dimensional errors are usually assumed to follow a normal distribution, and the 3σ principle is widely used in quality control [3]; however, other distributions may appear, such as a uniform distribution or a triangular distribution. With geometric errors, the distributions are more varied, and are typically multi-dimensional and non-negative. Wu [4] used a Rayleigh distribution to model positional deviations. Braun [5] reported experimental studies that support non-normal statistical models for the tolerances of populations of parts. These studies showed that geometric errors follow a Rice distribution or non-central chi distribution in the absence of symmetric errors. However, to date, three-dimensional (3D) error distributions of positional tolerances applied to a point (i.e., the derived geometry of a spherical feature) have not been reported. Furthermore, the distributions of geometric errors with different dimensions and in the presence of symmetric errors have not been described in a unified manner.

Statistical measures of assemblability involve dimensional errors, as well as geometric errors describing the assembly of two parts. Shan [6] used feasible assembly formulae and Monte Carlo simulation to calculate the probability of successful two-hole and two-pin assemblies. Zou [7] reported a Gapspace-based model to assess assemblability statistically. Shen [8] proposed an improved simulation-based approach to evaluate the assemblability of multiple pin–hole floating mating geometries. Ameta [9, 10] extended the tolerance map to describe the probability of one-dimensional (1D) clearance in slot–tab and pin–hole assemblies. Dantan [11] used Monte Carlo methods to simulate geometric deviations via statistical tolerance analysis. These studies, however, did not consider the precedence or the constraints of the assembly sequence. These factors can lead to a change in the distribution of displacements and hence affect the assemblability.

The resulting error is given by the combined effects of several errors along propagation paths or dimensional chains, and its distribution will determine whether functional requirements are satisfied. To describe accumulated dimensional errors with non-normal distributions, Seo [12] used a three-level Taguchi-based three-point information method to achieve statistical tolerance analysis for general distribution. Lin [13] developed a beta distribution approximation method to describe error using a beta distribution. Varghese [14] utilized the probability distribution function for manufacturing data, together with a numerical method, to perform rapid statistical tolerance stack-up analyses. Similarly, Liu [15] used convolution to compute probability density functions to describe closed-loop components analytically. Tsai [16] proposed a moment-based method to compute the resultant tolerance to deal with non-normal error distributions with variance, skewness, and kurtosis. Kuo [17] employed the first four moments of a truncated normal distribution to carry out tolerance analysis of components with a doubly truncated normal distribution. Khodaygan [18] used statistical analysis of asymmetric tolerances based on fuzzy logic to represent the uncertainty of tolerance components. Although these methods are sufficiently flexible to deal with different kinds of distribution, they can only be applied to 1D geometric errors and are not suitable for multi-dimensional geometric errors. Whitney [19] and Ghie [20] proposed space-state- and Jacobian-matrix-based methods for statistical analysis of geometric tolerances. However, the assembly variation was simulated based on Monte Carlo methods rather than a direct relationship with the tolerances. Therefore, they were not able to validate the functional requirements and optimize tolerances due to the prohibitively large computational costs.

Here, we describe an analytical model used to predict assembly precision that can improve the efficiency of the analysis of geometric tolerances. The model can be used to obtain an assembly precision and assembly capability index rapidly, and is therefore useful for direct practical production, and can provide a reference for modifying the design parameters.

3 Unified error distributions of geometric tolerances

To implement the calculations of assembly precision, we require measurements of the directions of the deviations for various types of geometric tolerance. We then use these deviations to calculate transformation of the nominal position, i.e., we calculate the maximum distance from the nominal position using the measured geometric tolerance. The relationship between the geometric tolerance and the variance of each of the deviations can be obtained from the unified error distribution.

3.1 Deviation direction

When features or their derived geometries are constrained by geometric tolerances, points on them may deviate from their nominal position within a given tolerance. To express the position of each point, we should obtain the constraints that describe the directions of features.

In the design process of parts and assemblies, defined tolerances and assembly information are used to constrain variation among the features of a part or those of different parts. Commonly, more than two features are engaged in a single location scheme. As a result, the constrained directions of different pairs of features can be correlated. For constraint analysis, all relevant features must be collected as a set. However, due to the functional requirements, tolerance primitives, and datum precedence, not all of the deviation directions between two features can be addressed or need to be addressed. Some may even be constrained repeatedly, so that in some situations, only a subset of the apparent constraint directions needs to be constrained.

A design can be divided into several deviations along several orthogonal directions; these are termed *deviation directions* here. Since one point can move along up to three independent directions in a 3D space, the number of deviation vectors is $1 \le k \le 3$.

Geometric tolerances are applied to constrain the surface or derived geometry of a feature. For a surface, there is only one deviation direction, because it can only deviate from the nominal position as a whole within the tolerance zone. For a derived geometry, the number of deviation directions is equal to the number of degrees of freedom (DOFs) of translation; otherwise, the derived geometry remains invariant following the deviation. Table 1 lists the deviation directions for different types of feature that are constrained by different types of geometric tolerance.

It is possible that not all of the deviation directions of a feature are restricted by datum features or datum reference frames. Therefore, the number of deviation directions may be fewer than that listed in Table 1.

For example, as shown in Fig. 1, the axis of a cylindrical feature is restricted by datum plane A by the position tolerance. Rotation around Y and translation along X are constrained, and each point on the axis can deviate from the nominal position only in X; therefore, the number of deviation directions is one. From Table 1, we can see that up to two deviation directions can be constrained for a straight line; hence, the number of deviation directions is related to the datum reference frame.

3.2 Transfer of nominal position

For each deviation direction, among all the points on a feature or the derived geometry, the maximum distance from the nominal position affects the geometric tolerance. It has been shown [4, 5] that the deviations in different directions can be assumed to be independent and normally distributed.

Let l_q be the deviation along the qth direction. Because the manufacturing conditions are identical for each deviation direction, the deviations in different directions have the same variance σ_l^2. The distribution of l_q can then be expressed in a unified way as follows:

$$\mathrm{l_q} \sim N\left(\mu_\mathrm{q}, {\sigma_\mathrm{l}}^2\right) \quad (1 \le \mathrm{q} \le k) \tag{1}$$

Because of systematic errors, we typically do not have $\mu_q = 0$. As a result, the center of the distribution shifts from the nominal position. If we also shift the nominal position μ_q along the qth deviation direction, and use this as the new nominal position, the distributions of the deviations can be made symmetrical about the new nominal position.

Although the distributions of the deviations relative to the new and original nominal positions do not necessarily coincide, μ_q is typically so small (compared with the tolerance) that this difference can be neglected in practice. From the deviations along all directions relative to the new nominal position, we can obtain the geometric error T as follows:

$$\frac{T}{2} = \sqrt{\sum_{\mathrm{q}=1}^{k} \left(l_\mathrm{q} - \mu_\mathrm{q}\right)^2} \tag{2}$$

3.3 Unified error distribution

The distribution of the square root of the sum of squares of independent random variables that are normally distributed is termed the chi distribution (or χ distribution). Because the deviations in different directions are independent, we have

$$\frac{T}{2\sigma_l} = \sqrt{\sum_{\mathrm{q}=1}^{k} \left(\frac{l_\mathrm{q} - \mu_\mathrm{q}}{\sigma_l}\right)^2} \sim \chi(\mathrm{k}) \tag{3}$$

where $\chi(k)$ is the χ-distribution with k DOFs. Eq. (3) describes the unified error distribution of the geometric tolerances. Let μ_k be the expectation and σ_k be the variance; then, the expectation and variance of the geometric error satisfy:

$$\begin{cases} \dfrac{\mathrm{E}(T)}{2\sigma_\mathrm{l}} = \mu_k = \sqrt{2}\dfrac{\Gamma((k+1)/2)}{\Gamma(k/2)} \\ \dfrac{\mathrm{D}(T)}{4{\sigma_\mathrm{l}}^2} = {\sigma_k}^2 = k - {\mu_k}^2 \end{cases} \tag{4}$$

where $\Gamma(\cdot)$ is the gamma function. Table 2 lists values of μ_k and σ_k^2 when $k = 1$, 2, and 3.

Table 1 The deviation directions of different types of features and their derived geometries

Feature (derived geometry)	Form, profile, runout	Direction	Position
Plane (plane)	Normal direction k=1	Normal direction k=1	Normal direction k=1
Cylinder, cone (straight line)	Radius direction k=1 (perp. to axis k=2)	Perp.to axis k=2	Perp.to axis k=2
Sphere (point)	Radius direction k=1	None k=0	Any direction k=3

According to the six-sigma principle, to ensure an acceptable range of the geometric tolerance, the geometric tolerance should satisfy the following relationship:

$$\mathrm{t}-\mathrm{E}(T)=3\sqrt{\mathrm{D}(T)} \tag{5}$$

By combining this expression with Eqs. (4) and (5), the relationship between the geometric tolerance and the variance of each deviation is given by

$$\mathrm{t}=2(\mu_k+3\sigma_\mathrm{k})\sigma_\mathrm{l} \tag{6}$$

4 Statistical analysis of variation

Depending on the type of feature (i.e., plane, straight line, or point), the constraints of the deviation required to achieve tolerance may vary. We use the relationship between the maximum distance from the nominal position and the deviation direction to obtain the error distribution for each direction. The variance of the displacements under partially constrained conditions is obtained using analysis of variance (ANOVA).

4.1 Parametric modeling

Let $t_{i,j}$ be the geometric tolerance of the ith target feature relative to the jth datum feature. The tolerance is applied to the surface of the ith feature if j=0; otherwise, the tolerance is used to constrain the variation in the derived geometry. If a feature is a feature-of-size (FOS), the upper and lower limits of the deviation of its dimensions are represented by m_i and n_i, respectively. The length, width, height, and radius of the ith feature are represented by L_i, W_i, H_i, and R_i, respectively.

To carry out ANOVA of features, the variation in the ith feature relative to the jth feature (which is restricted by $t_{i,j}$) is described as

$$\delta \mathrm{v}_{i,j}=\left(\delta x_{i,j},\delta y_{i,j},\delta z_{i,j},\delta\alpha_{i,j},\delta\beta_{i,j},\delta\gamma_{i,j}\right) \tag{7}$$

where $\delta x_{i,j}$, $\delta y_{i,j}$, and $\delta z_{i,j}$ are the deviations in the X, Y, and Z axes, respectively, and $\delta\alpha_{i,j}$, $\delta\beta_{i,j}$ and $\delta\gamma_i$ are the deviations in the orientation around the X, Y, and Z axes, respectively. These deviations can be assumed to be independent and normally distributed, as has been shown using the central limit theorem [19]. The expectation values relative to the original and new nominal positions are described by

$$\begin{cases} E_0(\delta \mathrm{v}_{i,j})=\left(E_0(\delta x_{i,j}),E_0\left(\delta y_{i,j}\right),E_0(\delta z_{i,j}),E_0(\delta\alpha_{i,j}),E_0(\delta\beta_{i,j}),E_0\left(\delta\gamma_{i,j}\right)\right) \\ E(\delta \mathrm{v}_{i,j})=\left(E(\delta x_{i,j}),E\left(\delta y_{i,j}\right),E(\delta z_{i,j}),E(\delta\alpha_{i,j}),E(\delta\beta_{i,j}),E\left(\delta\gamma_{i,j}\right)\right) \end{cases} \tag{8}$$

The deviations of the farthest point from the new nominal position along X, Y, and Z are represented by $\Delta x_{i,j}$, $\Delta y_{i,j}$, and $\Delta z_{i,j}$, respectively, which are normally distributed with the same variances $\sigma_{i,j}{}^2$, i.e.,

$$\begin{cases} \Delta x_{i,j}\sim N\left(0,\sigma_{i,j}{}^2\right) \\ \Delta y_{i,j}\sim N\left(0,\sigma_{i,j}{}^2\right) \\ \Delta z_{i,j}\sim N\left(0,\sigma_{i,j}{}^2\right) \end{cases} \tag{9}$$

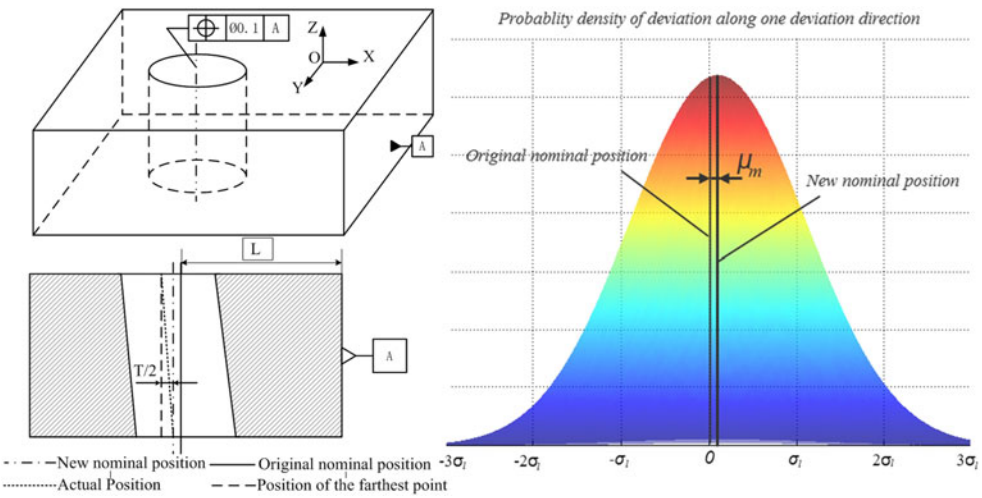

Fig. 1 The deviation directions of the position tolerance for a hole, and the distribution of the deviations along one deviation direction

Table 2 The expectation values and the variance of the χ distribution with k degrees of freedom

k	1	2	3
μ_k	(2/π)1/2	(π/2)1/2	(8/π)1/2
σ_k^2	1–2/π	2-π/2	3–8/π

Using Eq. (6), $\sigma_{i,j}^2$ can be expressed in term of $t_{i,j}$, i.e.,

$$\sigma_{i,j}^2 = \frac{t_{i,j}^2}{4(\mu_k + 3\sigma_k)^2} \tag{10}$$

4.2 Variation in a plane

A plane can be constrained along its normal direction (the Z axis) and in two orthogonal directions parallel to the plane (i.e., the X and Y axes). Based on the shape of the boundary, a plane can be categorized as either circular or rectangular.

We can represent a rectangular plane by using the central points along the four sides A, B, C, and D, as shown in Fig. 2. Variations in such a plane will make these points deviate from the nominal positions in the Z axis by z_A, z_B, z_C, and z_D, which can be calculated in term of the displacement of the plane as follows:

$$\begin{cases} z_A = \delta z_{i,j} - L_i \delta\beta_{i,j}/2 \\ z_B = \delta z_{i,j} + L_i \delta\beta_{i,j}/2 \\ z_C = \delta z_{i,j} - W_i \delta\alpha_{i,j}/2 \\ z_D = \delta z_{i,j} + W_i \delta\alpha_{i,j}/2 \end{cases} \tag{11}$$

Because all possible positions of these central points are symmetrical about the new nominal position, their expectation values are zero. Hence, using Eq. (11) to express the displacements in term of the deviations of the central points, the expectation values of the displacements can be expressed as

$$\begin{cases} E(\delta z_{i,j}) = E((z_A + z_B)/2) = E((z_C + z_D)/2) = 0 \\ E(\delta\alpha_{i,j}) = E((z_D - z_C)/W_{i,j}) = 0 \\ E(\delta\beta_{i,j}) = E((z_B - z_A)/L_{i,j}) = 0 \end{cases} \tag{12}$$

From Eq. (11), deviations in A and B are related only to the displacements around Y and along Z. Furthermore, the plane can be located within the tolerance zone wherever the two points are. Therefore, deviations in A and B are irrelevant, and the covariance of z_A and z_B is given by the following:

$$\begin{aligned} &Cov(z_A, z_B) = E(z_A z_B) - E(z_A)E(z_B) \\ &= E\left(\delta z_{i,j}^2 - L_i^2 \delta\beta_{i,j}^2/4\right) - 0 \times 0 \\ &= D(\delta z_{i,j}) + E^2(\delta z_{i,j}) - D(\delta\beta_{i,j} L_i/2) - E^2(\delta\beta_{i,j} L_i/2) \\ &= D(\delta z_{i,j}) - D(\delta\beta_{i,j} L_i/2) = 0 \end{aligned} \tag{13}$$

and consequently, the variances in the displacements around Y and along Z satisfy the following relationship:

$$D(\delta z_{i,j}) = L_i^2 D(\delta\beta_{i,j})/4 \tag{14}$$

Similarly, from the deviations in the central points C and D, the variances of the displacements around X and along Z are described by

$$D(\delta z_{i,j}) = W_i^2 D(\delta\alpha_{i,j})/4 \tag{15}$$

On a rectangular plane, one or more of the four vertexes will be farthest from the new nominal position, which determines the deviation along the only available deviation direction of the plane. $\Delta z_{i,j}$ can therefore be obtained from the displacements of the plane as follows:

$$|\Delta z_{i,j}| = |\delta z_{i,j}| + L_i |\delta\beta_{i,j}|/2 + W_i |\delta\alpha_{i,j}|/2 \tag{16}$$

For independent variables ($x_1, x_2 \ldots, x_a, y_1, y_2, \ldots, y_b$), if $h(\cdot)$ and $g(\cdot)$ are continuous functions, it follows that $h(x_1, x_2 \ldots, x_a)$ and $g(y_1, y_2, \ldots, y_b)$ are independent. It also follows that $|\delta z_{i,j}|$, $|\delta\alpha_{i,j}|$, and $|\delta\beta_{i,j}|$ are independent because $\delta z_{i,j}$, $\delta\alpha_{i,j}$, and $\delta\beta_{i,j}$ are independent and $|\cdot|$ is a continuous function. From Eq. (16), the variance of $|\Delta z_{i,j}|$ can be calculated as follows:

$$\begin{aligned} D(|\Delta z_{i,j}|) &= D(|\delta z_{i,j}|) + L_i^2 D(|\delta\beta_{i,j}|)/4 \\ &\quad + W_i^2 D(|\delta\alpha_{i,j}|)/4 \end{aligned} \tag{17}$$

Since the expectation values of the displacements relative to the new nominal positions are zero (which follows from Eq. (12)), the absolute value of each

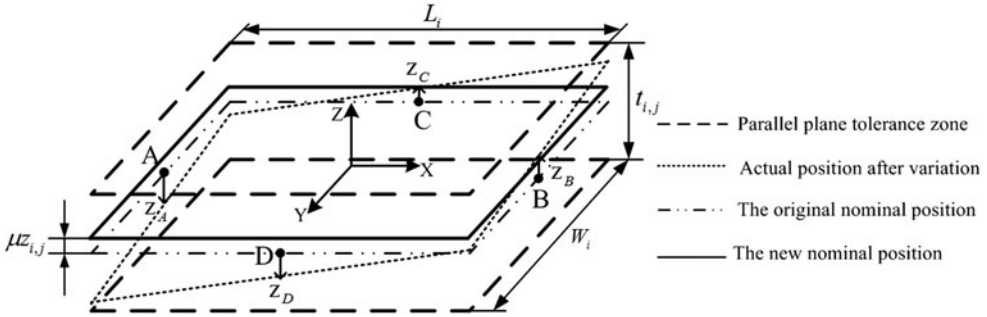

Fig. 2 The variation of a rectangular plane within the tolerance zone between two parallel planes

displacement follows a half-normal distribution, the variance of which can be expressed as

$$D(|\cdot|) = \left(1-\frac{2}{\pi}\right)D(\cdot) \tag{18}$$

Combining this expression with Eqs. (14), (15), (17), and (18), the variances of all displacements of the rectangular plane can be expressed as

$$\begin{cases} D(\delta z_{i,j}) = {\sigma_{i.j}}^2/3 \\ D(\delta\alpha_{i,j}) = 4{\sigma_{i.j}}^2/3{W_i}^2 \\ D(\delta\beta_{i,j}) = 4{\sigma_{i.j}}^2/3{L_i}^2 \end{cases} \tag{19}$$

However, sometimes, some apparently constrained directions may not be restricted, and the distribution of $\Delta z_{i,j}$ remains invariant, yet the distributions of displacements along or around the constrained directions may still change. Table 3 lists the variances of the displacements under such partially constrained conditions.

We may describe a round plane using four endpoints along the X and Y axis, A, B, C, and D, as shown in Fig. 3, where z_A, z_B, z_C, and z_D are the deviations in the Z axis relative to the new nominal position. From the ANOVA for a rectangular plane, we can obtain the expectation values and variances of the displacements of a round plane as follows:

$$\begin{cases} E(\delta z_{i,j}) = E(\delta\beta_{i,j}) = E(\delta\alpha_{i,j}) = 0 \\ D(\delta z_{i,j}) = {R_i}^2 D(\delta\alpha_{i,j}) = {R_i}^2 D(\delta\beta_{i,j}) \end{cases} \tag{20}$$

In contrast to a rectangular plane, the points on the boundary of a circular plane will deviate from the new nominal positions equally. From the relationship between the coordinates of a point and its deviation, $\Delta z_{i,j}$ can be expressed in terms of the displacements as follows:

$$|\Delta z_{i,j}| = |\delta z_{i,j}| + R_i\sqrt{{\delta\alpha_{i,j}}^2 + {\delta\beta_{i,j}}^2} \tag{21}$$

Similarly, because of the independence of the displacements, it follows that

$$D(|\Delta z_{i,j}|) = D(|\delta z_{i,j}|) + {R_i}^2 D\left(\sqrt{{\delta\alpha_{i,j}}^2 + {\delta\beta_{i,j}}^2}\right) \tag{22}$$

Table 3 The variances of displacements with partially constrained directions for a rectangular plane

Constraint direction (s)	$D(\delta z_{i,j})$	$D(\delta\alpha_{i,j})$	$D(\delta\beta_{i,j})$
$\alpha_{i,j}$, $\beta_{i,j}$	0	$2{\sigma_{i,j}}^2/{W_i}^2$	$2{\sigma_{i,j}}^2/{L_i}^2$
$z_{i,j}$, $\alpha_{i,j}$	${\sigma_{i,j}}^2/2$	$2{\sigma_{i,j}}^2/{W_i}^2$	0
$z_{i,j}$, $\beta_{i,j}$	${\sigma_{i,j}}^2/2$	0	$2{\sigma_{i,j}}^2/{L_i}^2$
$z_{i,j}$	${\sigma_{i,j}}^2$	0	0
$\alpha_{i,j}$	0	$4{\sigma_{i,j}}^2/{W_i}^2$	0
$\beta_{i,j}$	0	0	$4{\sigma_{i,j}}^2/{L_i}^2$

Because $\delta\alpha_{i,j}$ and $\delta\beta_{i,j}$ are distributed normally and their expectation values are all zero, the second term on the right-hand side of Eq. (22) can be rewritten using Eq. (20), and the variance of the chi distribution with the 2 DOFs listed in Table 2, i.e.,

$${R_i}^2 D\left(\sqrt{{\delta\alpha_{i,j}}^2 + {\delta\beta_{i,j}}^2}\right) = {R_i}^2{\sigma_2}^2 D(\delta\alpha_{i,j}) \tag{23}$$

By combining this expression with Eqs. (18), (20), (22), and (23), the variances of the displacements can be expressed as

$$\begin{cases} D(\delta z_{i,j}) = \dfrac{2(\pi-2){\sigma_{i.j}}^2}{-\pi^2+6\pi-4} \\ D(\delta\alpha_{i,j}) = D(\delta\beta_{i,j}) = \dfrac{2(\pi-2){\sigma_{i.j}}^2}{(-\pi^2+6\pi-4){R_i}^2} \end{cases} \tag{24}$$

If only the partially constrained directions are restricted, the variances of the displacements along or around them are as listed in Table 4.

4.3 Variation in straight line

A straight line can be constrained along and around two orthogonal directions perpendicular to the line (i.e., X axis and Y axis). Let the points A and B be the two endpoints of the straight line, as shown in Fig. 4. Within the tolerance zone, the deviations of the two points in the X and Y axes can be represented by x_A, x_B, y_A, and y_B, which can be expressed in terms of the displacements of the straight line as follows:

$$\begin{cases} x_A = \delta x_{i,j} + H_i\delta\beta_{i,j}/2 \\ x_B = \delta x_{i,j} - H_i\delta\beta_{i,j}/2 \\ y_A = \delta y_{i,j} + H_i\delta\alpha_{i,j}/2 \\ y_B = \delta y_{i,j} - H_i\delta\alpha_{i,j}/2 \end{cases} \tag{25}$$

Because all of the possible positions of A and B along the X and Y axes are symmetric about the new nominal position, the expectation values of x_A, x_B, y_A, and y_B are all zero. Hence, the expectation values of the displacements relative to the new nominal position can be expressed as

$$\begin{cases} E(\delta x_{i,j}) = E[(x_A + x_B)/2] = 0 \\ E(\delta y_{i,j}) = E[(y_A + y_B)/2] = 0 \\ E(\delta\alpha_{i,j}) = E[(y_B - y_A)/H_i] = 0 \\ E(\delta\beta_{i,j}) = E[(x_B - x_A)/H_i] = 0 \end{cases} \tag{26}$$

Moreover, regardless of the location of points A and B along the X axis, we can guarantee that the axis is located within the tolerance zone; therefore, x_A and x_B

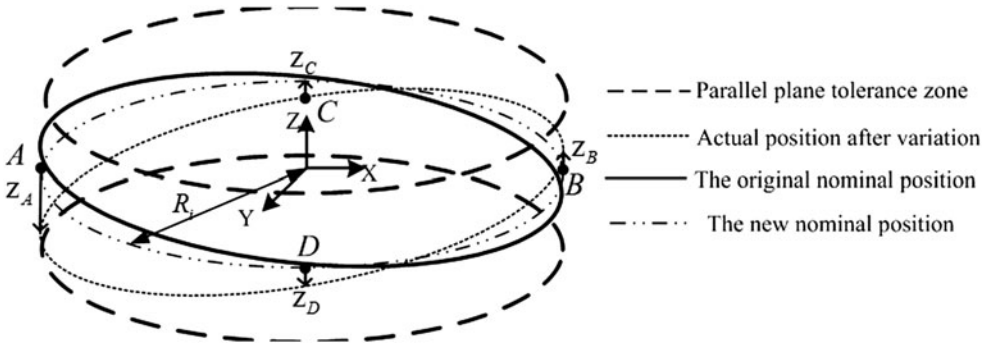

Fig. 3 The variation of a circular plane within the tolerance zone between two parallel planes

are irrelevant. As a result, from the covariance of x_A and x_B, it follows that

$$\begin{aligned} &Cov(x_A, x_B) = E(x_A x_B) - E(x_A)E(x_B) \\ &= E\left(\delta x_{i,j}{}^2 - H_i{}^2 \delta\beta_{i,j}{}^2/4\right) - 0 \times 0 \\ &= D\left(\delta x_{i,j}\right) + E^2\left(\delta x_{i,j}\right) - D\left(\delta\beta_{i,j} H_i/2\right) - E^2\left(\delta\beta_{i,j} H_i/2\right) \\ &= D\left(\delta x_{i,j}\right) - D\left(\delta\beta_{i,j} H_i/2\right) = 0 \end{aligned} \tag{27}$$

From Eq. (27), the variances of the displacements along X and around Y satisfy the following relationship:

$$D\left(\delta x_{i,j}\right) = H_i{}^2 D\left(\delta\beta_{i,j}\right)/4 \tag{28}$$

Similarly, the variances of displacements along Y and around X have the following relationship:

$$D\left(\delta y_{i,j}\right) = H_i{}^2 D\left(\delta\alpha_{i,j}\right)/4 \tag{29}$$

For each deviation direction, one of the two endpoints will be the farthest point from the new nominal position. Therefore, based on the coordinates and deviations of A and B, $\Delta x_{i,j}$ and $\Delta y_{i,j}$ can be computed as follows:

$$\begin{cases} \left|\Delta x_{i,j} - \delta x_{i,j}\right| = \left|H_i \delta\beta_{i,j}/2\right| \\ \left|\Delta y_{i,j} - \delta y_{i,j}\right| = \left|H_i \delta\alpha_{i,j}/2\right| \end{cases} \tag{30}$$

Table 4 The variances of displacements with partially constrained directions for a circular plane

Constraint direction(s)	$D\ (\delta z_{i,j})$	$D\ (\delta\alpha_{i,j})$	$D\ (\delta\beta_{i,j})$
α, β	0	$\frac{2(\pi-2)\sigma_{i,j}{}^2}{\pi(4-\pi)R_i{}^2}$	$\frac{2(\pi-2)\sigma_{i,j}{}^2}{\pi(4-\pi)R_i{}^2}$
z, α	$\sigma_{i,j}{}^2/2$	$2\sigma_{i,j}{}^2/R_i{}^2$	0
z, β	$\sigma_{i,j}{}^2/2$	0	$2\sigma_{i,j}{}^2/R_i{}^2$
z	$\sigma_{i,j}{}^2$	0	0
α	0	$\sigma_{i,j}{}^2/R_i{}^2$	0
β	0	0	$\sigma_{i,j}{}^2/R_i{}^2$

Since all parameters are normally distributed, and their expectation values are zero, from Eq. (17) it follows that

$$\begin{cases} \mathrm{D}\left(\Delta x_{i,j} - \delta x_{i,j}\right) = \mathrm{D}\left(H_i \delta\beta_{i,j}/2\right) = \mathrm{D}\left(\Delta x_{i,j}\right) + \mathrm{D}\left(\delta x_{i,j}\right) - 2\mathrm{Cov}\left(\Delta x_{i,j}, \delta x_{i,j}\right) \\ \mathrm{D}\left(\Delta y_{i,j} - \delta y_{i,j}\right) = \mathrm{D}\left(H_i \delta\alpha_{i,j}/2\right) = \mathrm{D}\left(\Delta y_{i,j}\right) + \mathrm{D}\left(\delta y_{i,j}\right) - 2\mathrm{Cov}\left(\Delta y_{i,j}, \delta y_{i,j}\right) \end{cases} \tag{31}$$

The probabilities that the endpoints A and B are the farthest point are equal. Therefore, and from Eqs. (26) and (30), $Cov(\Delta x_{i,j}, \delta x_{i,j})$ and $Cov(\Delta y_{i,j}, \delta y_{i,j})$ can be simplified to

$$\begin{cases} \mathrm{Cov}\left(\Delta x_{i,j}, \delta x_{i,j}\right) = E\left[\left(\Delta x_{i,j} - E\left(\Delta x_{i,j}\right)\right)\left(\delta x_{i,j} - E\left(\Delta\delta x_{i,j}\right)\right)\right] = E\left[\Delta x_{i,j}\delta x_{i,j}\right] \\ \quad = E\left[\delta x_{i,j}{}^2 \pm H_i \delta\beta_{i,j}\delta x_{i,j}/2\right] = E\left(\delta x_{i,j}{}^2\right) \pm E\left(\delta x_{i,j}\right)E\left(H_i\delta\beta_{i,j}/2\right) = D\left(\delta x_{i,j}\right) \\ \mathrm{Cov}\left(\Delta y_{i,j}, \delta y_{i,j}\right) = E\left[\left(\Delta y_{i,j} - E\left(\Delta y_{i,j}\right)\right)\left(\delta y_{i,j} - E\left(\Delta\delta y_{i,j}\right)\right)\right] = E\left[\Delta y_{i,j}\delta y_{i,j}\right] \\ \quad = E\left[\delta y_{i,j}{}^2 \pm H_i \delta\alpha_{i,j}\delta y_{i,j}/2\right] = E\left(\delta y_{i,j}{}^2\right) \pm E\left(\delta y_{i,j}\right)E\left(H_i\delta\alpha_{i,j}/2\right) = D\left(\delta y_{i,j}\right) \end{cases} \tag{32}$$

Combining this expression with Eqs. (31) and (32), we can obtain the variances of $\Delta x_{i,j}$ and $\Delta y_{i,j}$ as follows:

$$\begin{cases} \mathrm{D}\left(\Delta x_{i,j}\right) = D\left(\delta x_{i,j}\right) + D\left(H_i \delta\beta_{i,j}/2\right) \\ \mathrm{D}\left(\Delta y_{i,j}\right) = D\left(\delta y_{i,j}\right) + D\left(H_i \delta\alpha_{i,j}/2\right) \end{cases} \tag{33}$$

Using Eqs. (28), (29), and (33), the variances of all displacements can be expressed as

$$\begin{cases} D\left(\delta x_{i,j}\right) = D\left(\delta y_{i,j}\right) = \sigma_{i.j}{}^2/2 \\ D\left(\delta\alpha_{i,j}\right) = D\left(\delta\beta_{i,j}\right) = 2\sigma_{i.j}{}^2/H_i{}^2 \end{cases} \tag{34}$$

If this expression is not satisfied, all of the constrained directions are restricted in one deviation direction, and the variances of the displacements along or around the restricted directions will change, as listed in Table 5.

4.4 Variation in a point

One point can be constrained along three directions (i.e., the X, Y, and Z axes), as shown in Fig. 5, where each direction

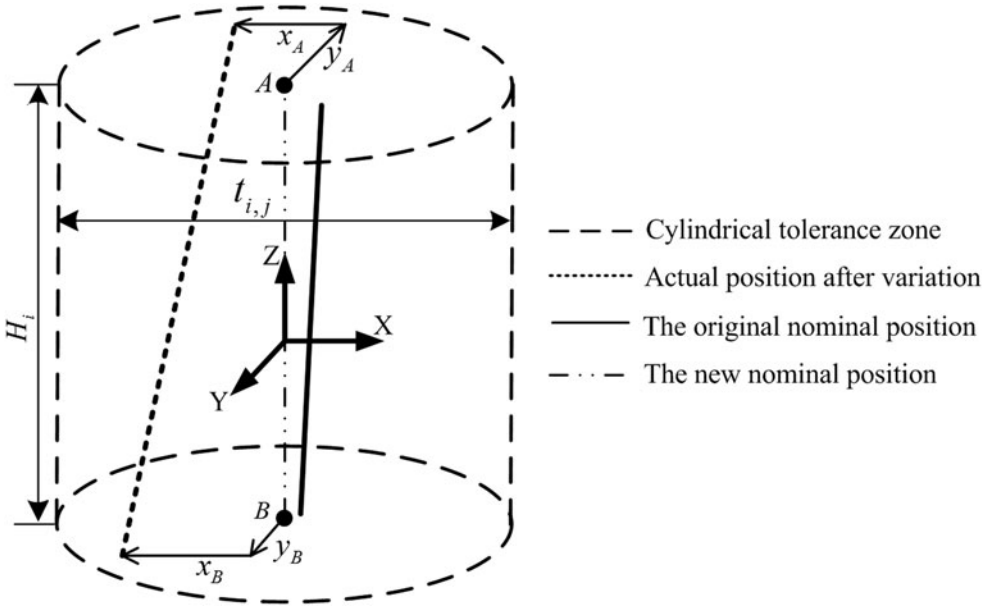

Fig. 4 The variation of a straight line within a cylindrical tolerance zone

corresponds to one deviation direction. Let x_O, y_O, and z_O be the deviations of a point O along the X, Y and Z axes; the deviations in each deviation direction and the displacement of point O within the tolerance zone can be expressed as follows:

$$\begin{cases} x_O = \delta x_{i,j} = \Delta x_{i,j} \\ y_O = \delta y_{i,j} = \Delta y_{i,j} \\ z_O = \delta z_{i,j} = \Delta z_{i,j} \end{cases} \tag{35}$$

Because the deviations of the point are symmetrical about the new nominal position, from Eq. (33), the expectation value of the displacements can expressed as

$$\begin{cases} E\left(\delta x_{i,j}\right) = E(x_O) = 0 \\ E\left(\delta y_{i,j}\right) = E(y_O) = 0 \\ E\left(\delta z_{i,j}\right) = E(z_O) = 0 \end{cases} \tag{36}$$

The variances of all displacements can be expressed as

$$\begin{cases} \mathrm{D}\left(\delta x_{i,j}\right) = D\left(\Delta x_{i,j}\right) = {\sigma_{i,j}}^2 \\ \mathrm{D}\left(\delta y_{i,j}\right) = D\left(\Delta x_{i,j}\right) = {\sigma_{i,j}}^2 \\ \mathrm{D}\left(\delta z_{i,j}\right) = D\left(\Delta z_{i,j}\right) = {\sigma_{i,j}}^2 \end{cases} \tag{37}$$

The variance of the displacement of the unconstrained directions will be therefore be zero.

5 Analytical model of assembly variation

The precedence of the relative positions of a pin–hole assembly may vary depending on the results of a statistical analysis of geometric variation. Considering the covariance of the accumulated variation during assembly, a relationship can be constructed between the unified error distribution and the assembly precision, which allows us to calculate an assembly capability index efficiently.

5.1 Variation in the clearance fit

During assembly, if we assimilate the assembly features as the data and target features of a geometric tolerance, the gap between the assembly features can be viewed as a geometric tolerance. However, this gap may vary due to size and form tolerances. To cover the worst-case scenario, the geometric tolerance should be equal to the maximum gap.

Because the possible directions and positions of one assembly feature are symmetric about another following mating, the expectation values of all displacements are zero. Based on the precedence of assembly constraints between two parts, we can establish a procedure to analyze the variances of the displacements induced by the clearance fits, as shown by the flowchart in Fig. 6.

Table 5 The variances of displacements with partially constrained directions for a circular plane

Deviation direction, X			Deviation direction, Y		
Constraint direction(s)	$D\ (\delta x_{i,j})$	$D\ (\delta \alpha_{i,j})$	Constraint direction(s)	$D\ (\delta y_{i,j})$	$D\ (\delta \alpha_{i,j})$
$x_{i,j}$, $\beta_{i,j}$	${\sigma_{i,j}}^2/2$	$2{\sigma_{i,j}}^2/H_i^2$	$y_{i,j}$, $\alpha_{i,j}$	${\sigma_{i,j}}^2/2$	$2{\sigma_{i,j}}^2/H_i^2$
$x_{i,j}$	${\sigma_{i,j}}^2$	0	$y_{i,j}$	${\sigma_{i,j}}^2$	0
$\beta_{i,j}$	0	$4{\sigma_{i,j}}^2/H_i^2$	$\alpha_{i,j}$	0	$4{\sigma_{i,j}}^2/H_i^2$

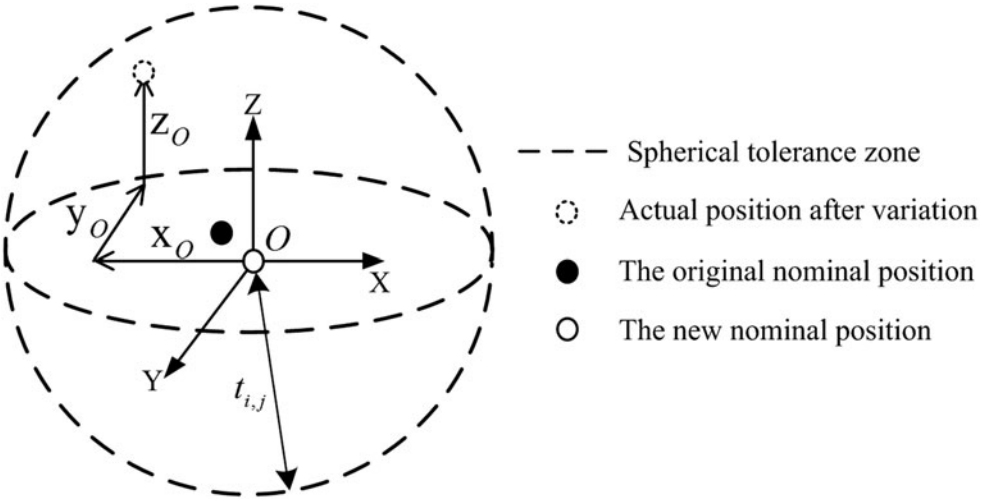

Fig. 5 The variation of a point within a spherical tolerance zone

When an assembly constraint of a clearance fit has the highest precedence, none of the constrained directions has been restricted previously, and the variances of the displacements can be obtained directly based on the equivalent geometric tolerances of the clearance fit and the statistical analysis of the variations given above. Otherwise, the partially constrained directions have been restricted by other assembly constraints that have higher precedence. The variances of the displacements along or around the unconstrained directions are determined by equivalent geometric tolerance of the clearance fit, whereas the variances of the constrained displacements are determined by the geometric tolerances between the assembly features of one part.

Here, we take the pin–hole assembly shown in Fig. 7 as an example. The *i*th feature corresponds to a pin, and the *j*th feature corresponds to a hole. The equivalent geometric tolerance of the clearance fit is as follows:

$$\mathrm{t}_{i,j} = \mathrm{n}_j - \mathrm{m}_i \tag{38}$$

As shown in the upper-right of Fig. 7, the assembly constraints of the pin–hole have the highest precedence, so there are no constrained directions that have been restricted previously. Variances of the displacements due to the clearance fit can be calculated directly using Eqs. (10) and (34).

$$\begin{cases} D(\delta x_{i,j}) = D\left(\delta y_{i,j}\right) = \dfrac{(\mathrm{c}_i - \mathrm{d}_j)^2}{8(\mu_2 + 3\sigma_2)^2} \\ D(\delta\alpha_{i,j}) = D(\delta\beta_{i,j}) = \dfrac{(\mathrm{c}_i - \mathrm{d}_j)^2}{2(\mu_2 + 3\sigma_2)^2 H_i^2} \end{cases} \tag{39}$$

Otherwise, some directions were restricted, as shown in the lower-right of Fig. 7, where the displacements around the *X* and *Y* axes of the pin and hole have been fixed due to assembly constraints of two planar features (the *i*'th and *j*'th features). Then, the pin–hole assembly restricts displacement only along the *X* and *Y* axes, the variances of which can be obtained according to Eqs. (10), (31) and (38), i.e.,

$$\begin{cases} D(\delta x_{i,j}) = D(\Delta x_{i,j}) - D\left(\dfrac{H_i}{2}(\delta\beta_{i,i'} - \delta\beta_{j,j'})\right) \\ \qquad = \dfrac{(\mathrm{c}_i - \mathrm{d}_j)^2}{4(\mu_2 + 3\sigma_2)^2} - \dfrac{H_i^2}{4}\left[D(\delta\beta_{i,i'}) + D(\delta\beta_{j,j'})\right] \\ D\left(\delta y_{i,j}\right) = D\left(\Delta y_{i,j}\right) - D\left(\dfrac{H_i}{2}(\delta\alpha_{i,i'} - \delta\alpha_{j,j'})\right) \\ \qquad = \dfrac{(\mathrm{c}_i - \mathrm{d}_j)^2}{4(\mu_2 + 3\sigma_2)^2} - \dfrac{H_i^2}{4}\left[D(\delta\alpha_{i,i'}) + D(\delta\alpha_{j,j'})\right] \end{cases} \tag{40}$$

5.2 Analytical model

Variations in the assembly reflect the displacements of the functional target features relative to the original nominal positions, as determined by the functional datum feature. Based on the linear accumulation model of assembly variation proposed by Zhou [21], the assembly variation can be expressed in terms of the displacements of the features as follows:

$$U_{6\times1} = A_{6\times q} V_{q\times1} \Leftrightarrow \begin{bmatrix} \delta x_f \\ \delta y_f \\ \delta z_f \\ \delta\alpha_f \\ \delta\beta_f \\ \delta\gamma_f \end{bmatrix} = A_{6\times q} \begin{bmatrix} \vdots \\ \delta x_{i,j} \\ \delta y_{i,j} \\ \delta z_{i,j} \\ \delta\alpha_{i,j} \\ \delta\beta_{i,j} \\ \delta\gamma_{i,j} \\ \vdots \end{bmatrix}_{q\times1} \tag{41}$$

where *U* is a matrix constructed from the displacements of a functional target feature (δx_f, δy_f, δz_f, $\delta\alpha_f$, $\delta\beta_f$, and $\delta\gamma_f$) relative

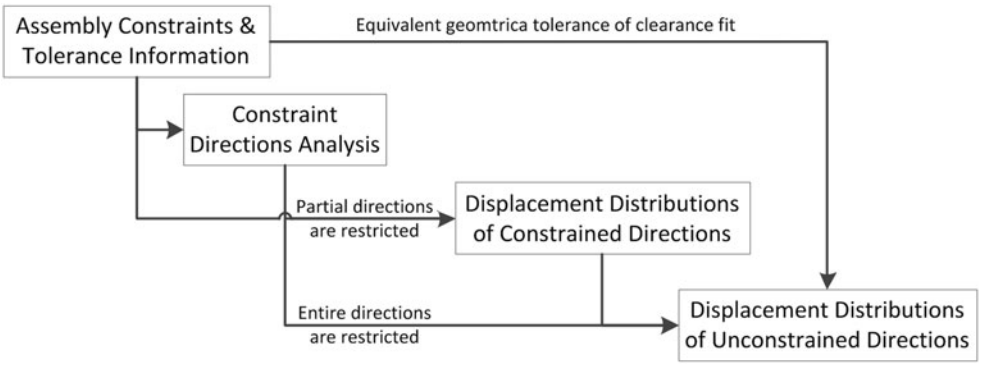

Fig. 6 A flowchart showing the analysis process for the variation of a clearance fit

to a functional datum feature, V is a matrix constructed using the relative displacements of features, which can be represented by q, and A is a coefficient matrix determined by the nominal positions of features.

The functional requirements are typically verified based on the deviations of several control points on the corresponding functional target features. Therefore, it is necessary to calculate the deviation of each control point with assembly variation, i.e.,

$$F_{p\times 1} = B_{p\times 6}U_{6\times 1} \Leftrightarrow \begin{bmatrix} l_1 \\ \vdots \\ l_p \end{bmatrix} = B_{p\times 6}\begin{bmatrix} \delta x_f \\ \delta y_f \\ \delta z_f \\ \delta \alpha_f \\ \delta \beta_f \\ \delta \gamma_f \end{bmatrix} \tag{42}$$

where F is a matrix describing the deviations of one control point, l_p represents the deviation along the pth deviation direction, and B is a coefficient matrix determined by the coordinates of the control point in the coordinate system of the functional target feature.

When varying the nominal positions of features, the nominal position of the control point on the functional target feature will also vary. Since the new nominal positions of features are determined by their displacement relative to the original nominal position, the deviations of the expectation values of the control point can be obtained from Eqs. (8), (41), and (42) as follows:

$$E_0(F) = \begin{bmatrix} E_0(l_1) \\ \vdots \\ E_0(l_p) \end{bmatrix} = E_0(BU) = E_0[B(AV)] = BAE_0(V) \tag{43}$$

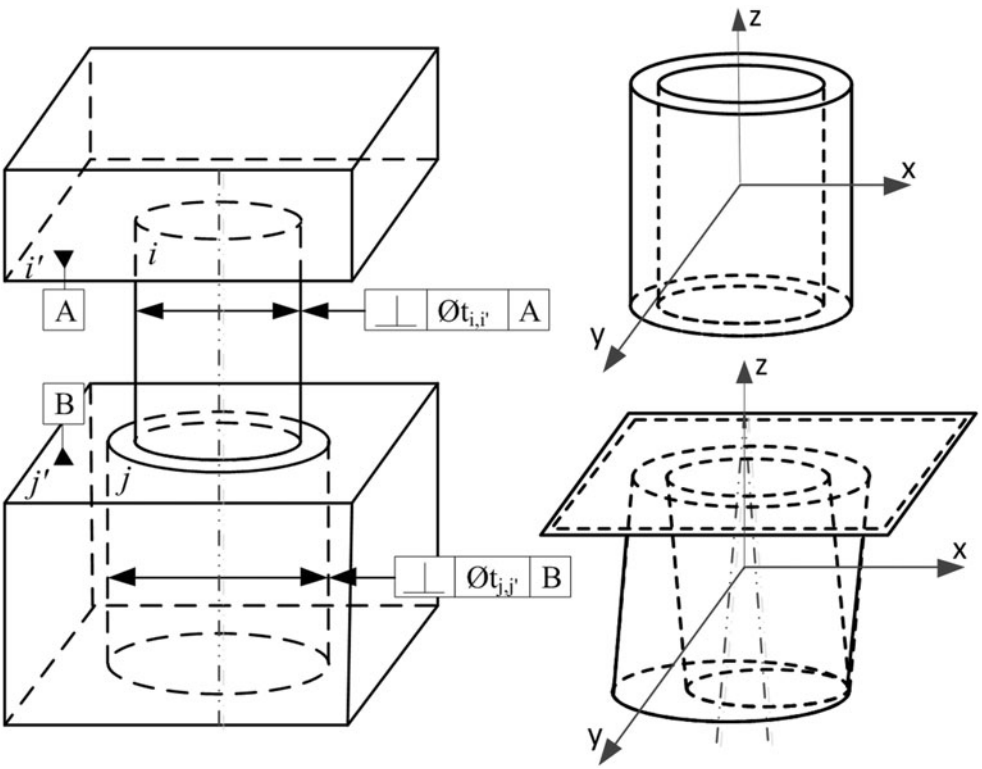

Fig. 7 The relative positions of pin–hole assemblies with various differing precedences

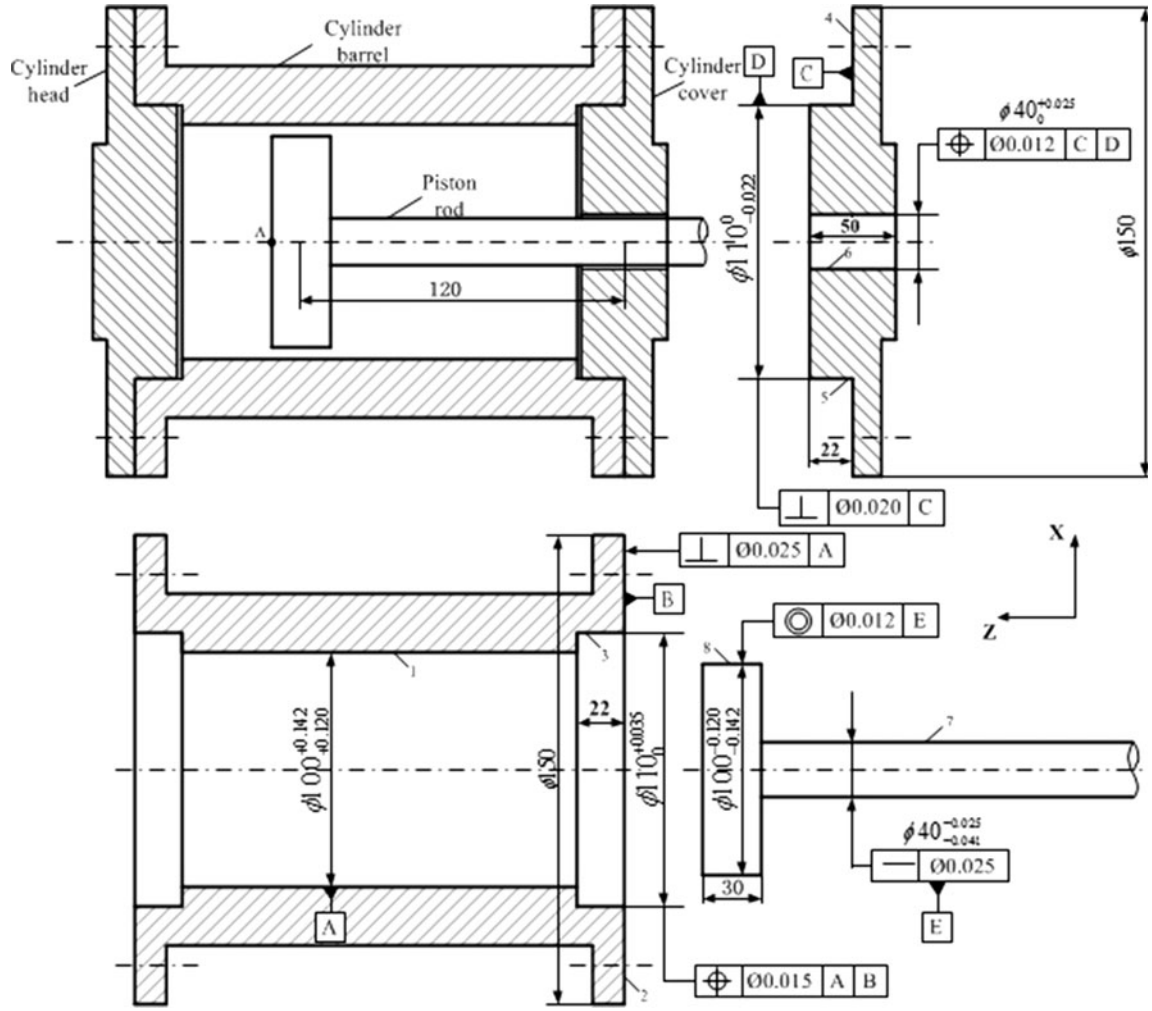

Fig. 8 The design of a single-rod piston cylinder, showing the tolerances

The variance of the deviation of the control point can be calculated using the covariance as follows:

$$\mathrm{Cov}(F)=\begin{bmatrix} D(l_1) & \cdots & \mathrm{Cov}(l_1,l_p) \\ \vdots & \ddots & \vdots \\ \mathrm{Cov}(l_p,l_1) & \cdots & D(l_p) \end{bmatrix}=\mathrm{Cov}(BU)=B\mathrm{Cov}(U)B^T \tag{44}$$
$$=B\mathrm{Cov}(AV)B^T=BA\mathrm{Cov}(V)A^TB^T=(BA)\mathrm{Cov}(V)(BA)^T$$

where Cov(V) is a diagonal matrix, since all displacements are independent, and where each diagonal element corresponds to the variance of one displacement. In particular, although a change in the nominal position of features will alter the coefficient matrix A, it will be too small to significantly affect the final assembly variation. Hence, A will remain invariant wherever new nominal positions occur.

In summary, Eqs. (43) and (44) constitute an analytical model of assembly variation, and the expectation values of deviation, and the variances of a control point can be obtained using this model.

5.3 Evaluation for the process capability index of an assembly

When one control point has two or three deviation directions, the deviations along them may not be independent following the accumulation of errors. Using principle component analysis (PCA), the eigenvectors of Cov(F) indicate the independent directions of deviations. Furthermore, the eigenvalues of Cov(F) are equal to the variances of the deviations along the directions of the eigenvectors. Let d_p and v_p represent the pth eigenvalue and eigenvector of Cov(F), respectively; it follows that

$$Cov(F)v_p=d_pv_p \tag{45}$$

For each direction of each eigenvector, the expectation value of the deviation, denoted e_p, can be determined from the following transformation:

$$e_p=\left|E_0(l_p)\right|\frac{E_0(l_p)\cdot v_p}{\left|E_0(l_p)\right|\times|v_p|}=\frac{E_0(l_p)\cdot v_p}{|v_p|} \tag{46}$$

Table 6 The expectation values and variances of the displacements among features

No.	$\delta v_{i,j}$	Expectation (mm/rad)	Variance (mm^2/rad^2)	No.	$\delta v_{i,j}$	Expectation (mm/rad)	Variance (mm^2/rad^2)
1	$\delta\alpha_{2,1}$	0.025/15/150	6.5975056×10^{-9}	11	$\delta x_{6,5}$	0.012/15	2.7879743×10^{-6}
2	$\delta\beta_{2,1}$	0.025/15/150	6.5975056×10^{-9}	12	$\delta y_{6,5}$	0.012/15	2.7879743×10^{-6}
3	$\delta x_{3,1}$	0.015/15	4.3562098×10^{-6}	13	$\delta x_{7,6}$	0	3.2545717×10^{-5}
4	$\delta y_{3,1}$	0.015/15	4.3562098×10^{-6}	14	$\delta y_{7,6}$	0	3.2545717×10^{-5}
5	$\delta\alpha_{4,2}$	0	0	15	$\delta\alpha_{7,6}$	0	5.2073164×10^{-8}
6	$\delta\beta_{4,2}$	0	0	16	$\delta\beta_{7,6}$	0	5.2073164×10^{-8}
7	$\delta x_{5,3}$	0	1.0596238×10^{-4}	17	$\delta x_{8,7}$	0.012/15	2.7879743×10^{-6}
8	$\delta y_{5,3}$	0	1.0596238×10^{-4}	18	$\delta y_{8,7}$	0.012/15	2.7879743×10^{-6}
9	$\delta\alpha_{6,4}$	0.012/15/50	4.4607588×10^{-9}	19	$\delta\alpha_{8,7}$	0.012/15/30	1.2390996×10^{-8}
10	$\delta\beta_{6,4}$	0.012/15/50	4.4607588×10^{-9}	20	$\delta\beta_{8,7}$	0.012/15/30	1.2390996×10^{-8}

Because the directions of the eigenvectors are independent, the functional requirements can be validated by comparing them with the largest range of deviations in these directions. If the functional requirements are denoted as T_f, the process capability index of the assembly, C_{pk}, can be evaluated as follows:

$$C_{pk} = \frac{T_f}{\mathrm{Max}\left[|e_p| + 3d_p\right]} \tag{47}$$

6 Example

To demonstrate the feasibility of our method, we consider a model of a single-rod piston cylinder, as shown in Fig. 8, as an example, and carry out a statistical tolerance analysis. The functional requirements of the piston cylinder are to guarantee that the gap between the two cylindrical surfaces (with nominal diameters of 100 mm) of the piston and the piston bore is at least 0.120 mm when the piston travel reaches the maximum distance of 120 mm. The point C on the axis of the piston is used as a control point.

We assume that the average systematic error is one fifteenth of the tolerance in each translation and orientation direction (multiplied by the dimensions of the feature). Based on the tolerance and dimensional information, the expectation values and variances of the displacements of features are listed in Table 6.

Using the dimensional information of the parts shown in Fig. 8, the following coefficient matrix A can be obtained:

$$A = \begin{bmatrix} 0 & 117 & 1 & 0 & 0 & 117 & 1 & 0 & 0 & 120 & 1 & 0 & 1 & 0 & 0 & 120 & 1 & 0 & 0 & 0 \\ -117 & 0 & 0 & 1 & -117 & 0 & 0 & 1 & -120 & 0 & 0 & 1 & 0 & 1 & -120 & 0 & 0 & 1 & 0 & 0 \\ 0 & 0 & 0 & 0 & 0 & 0 & 0 & 0 & 0 & 0 & 0 & 0 & 0 & 0 & 0 & 0 & 0 & 0 & 0 & 0 \\ 1 & 0 & 0 & 0 & 1 & 0 & 0 & 0 & 1 & 0 & 0 & 0 & 0 & 0 & 1 & 0 & 0 & 0 & 1 & 0 \\ 0 & 1 & 0 & 0 & 0 & 1 & 0 & 0 & 0 & 1 & 0 & 0 & 0 & 0 & 0 & 1 & 0 & 0 & 0 & 1 \\ 0 & 0 & 0 & 0 & 0 & 0 & 0 & 0 & 0 & 0 & 0 & 0 & 0 & 0 & 0 & 0 & 0 & 0 & 0 & 0 \end{bmatrix} \tag{48}$$

where each column in matrix A corresponds to an item in Table 6. Based on the coordinates of the control point C on the cylindrical feature of the piston, the following coefficient matrix B is obtained:

$$B = \begin{bmatrix} 1 & 0 & 0 & 0 & 15 & 0 \\ 0 & 1 & 0 & -15 & 0 & 0 \end{bmatrix} \tag{49}$$

The new nominal position of control point C relative to the original nominal position can then be calculated using Eq. (43), i.e.,

$$E_0(F) = \begin{bmatrix} 0.0066267 \\ -0.0014267 \end{bmatrix} \tag{50}$$

Table 7 The results of the analytical model described here and the results of other methods

Method	Deviation of axis (mm)	Process capability index
Worst case	0.14680	0.8174
Root sum square	0.06856	1.7503
Monte Carlo(10^5 times)	0.11201	1.0713
Analytical model	0.11465	1.0467

From Eq. (44), and the variances of the displacements of features listed in Table 6, the deviation covariance matrix of the control point is given by

$$\mathrm{Cov}(F) = \begin{bmatrix} 1.296514 \times 10^{-3} & 0 \\ 0 & 1.296514 \times 10^{-3} \end{bmatrix} \quad (51)$$

Because the covariance matrix is diagonal, the eigenvectors are the same as the deviation directions of the control point, and the eigenvalues are equal to the diagonal elements. From Eqs. (47), (50), and (51), the process capability index of the assembly is given by

$$C_{pk} = \frac{0.120}{0.0066267 + 3 \times \sqrt{1.296514 \times 10^{-3}}} = \frac{0.120}{0.11465} = 1.0467 \quad (52)$$

7 Results and discussion

Table 7 lists the results of analyses of the single-rod piston cylinder using the WC method, RSS method, the Monte Carlo method, and the analytical model described here. Compared with the Monte Carlo analysis, the WC method underestimated the process capability index and the RSS method overestimated the process capability index. These methods therefore do not provide an accurate measure of the process capability index; however, it can be computed quickly and directly based on tolerances and dimensional information. The results obtained using the analytical model described here were in good agreement with the results of the Monte Carlo method. It follows that our method has favorable accuracy compared with either the WC or RSS methods.

Although it has good accuracy, the Monte Carlo method incurs significant computational expense to obtain stable and accurate results. With a Monte Carlo approach, first, the tolerances are mapped to the constraint inequalities of the displacements. Second, each displacement is assigned independently and randomly based on a given distribution within the tolerance zone. Then, only if the selected displacements can satisfy the constraint inequalities, they will be utilized to accumulate the assembly variations. Hence, the actual distribution of the displacements is not the same as the given distribution. By contrast, with our model the distributions of the displacements are analyzed after ensuring that the geometric tolerances are satisfied. Then, using the expectation and covariance analysis based on linear accumulation of assembly variations, a direct relationship among the geometric tolerances and deviation variances of the control points can be established to verify the functional requirements. Therefore, our analytical model is considerably more efficient than the Monte Carlo method, with no significant loss of accuracy.

8 Conclusions and future work

We have described an analytical model to deal with statistical analyses of geometric tolerances efficiently and accurately. To express the error distributions of geometric tolerance, the deviation directions are summarized for different types of features, and the original nominal positions are transformed when systematic error is taken into consideration; the chi-distribution with a variable number of DOFs is used to describe a unified distribution of geometric errors. To analyze the assembly variation, direct relationships among the geometric tolerances, displacement distributions of features, and deviation distributions of control points are used to evaluate the functional requirements based on the tolerance. Moreover, partially constrained situations that arise due to datum precedence in geometric tolerances and assembly constraints are also considered in the model.

The method can be used to validate design schemes with geometric tolerances, and can also be used as part of optimization of geometric tolerances. It is advantageous to avoid wastage prior to assembly of parts, and our model has important theoretical and practical significance for decreasing product development times, reducing the cost of products, and improving the quality of products.

Some problems were not considered, such as where two parts are located by several coupled assembly features and displacement distributions. Through an analysis of the variations that are constrained by the location priority, constrained relationships among the variations of assembly features should be determined according to the contact conditions to achieve fits between opposed parallel planes, cylinders, cones, and spheres. We assumed that the displacements were normally distributed to establish the analytical model for geometric tolerances; however, in practice, the displacements may follow other distributions. Further work is therefore required to investigate the significance of coupled assembly features and of different distributions of displacements.

Acknowledgments This work was supported by National Natural Science Foundation of China under Grant No. 51275047.

References

1. Nigam SD, Turner JU (1995) Review of statistical approaches to tolerance analysis. CAD Comput Aided Des 27(1):6–15
2. Jami JJ, Ameta G, Zhengshu S (2007) Navigating the tolerance analysis maze. Comput-Aided Des Appl 4(5):705–718
3. Hong YS, Chang TC (2002) A comprehensive review of tolerancing research. Int J Prod Res 40(11):2425–2459
4. Wu Z, ElMaraghy WH, ElMaraghy HA (1988) Evaluation of cost-tolerance algorithms for design tolerance analysis and synthesis. Manuf Rev 1:168–179
5. Braun PR, Morse EP, Voelcker HB (1997) Research in statistical tolerancing: examples of intrinsic non-normalities and their effects. Proceeding of the 5th C1RP International Seminar on Computer-Aided Tolerancing, Toronto

6. Shan A, Roth RN, Wilson RJ (1999) A new approach to statistical geometrical tolerance analysis. Int J Adv Manuf Technol 15(3): 222–230
7. Zhihua Z, Morse EP (2003) Applications of the Gapspace model for mulitidimensional mechanical assemblies. ASME J Comput Inf Sci Eng 3(1):22–30
8. Shen Z, Shah JJ, Davidson JK (2005) Simulation-based tolerance and assemblablity analysis of assemblies with multiple pin/hole floating mating conditions. ASME
9. Ameta G, Davidson JK, Shah JJ (2007) Using Tolerance-Maps to generate frequency distribution of clearance for tab-slot assemblies. Proceeding of ASME IDETC/CIE, Las Vegas
10. Ameta G, Davidson JK, Shah JJ (2007) Using tolerance-maps to generate frequency distribution of clearance and allocate tolerances for pin-hole assemblies. J Comput Inf Sci Eng 7(4):347–359
11. Dantan J-Y, Qureshi A-J (2009) Worst-case and statistical tolerance analysis based on quantified constraint satisfaction problems and Monte Carlo simulation. Comput Aided Des 41(1):1–12
12. Seo HS, Kwak BM (2002) Efficient statistical tolerance analysis for general distributions using three-point information. Int J Prod Res 40(4):931–944
13. Lin S-S (1997) Statistical tolerance analysis based on beta distributions. J Manuf Syst 16(2):150–158
14. Varghese P, Braswell RN, Wang B (1996) Statistical tolerance analysis using FRPDF and numerical convolution. Comput Aided Des 28(9):723–732
15. Liu SG, Wang P, Li ZG (2008) Non-normal statistical tolerance analysis using analytical convolution method. J Adv Manuf Syst 7(1):127–130
16. Kuo C-H, Tsai J-C (2011) An analytical computation method for statistical tolerance analysis of assemblies with truncated normal mean shift. Int J Prod Res 49(7):1937–1955
17. Tsai JC, Kuo CH (2012) A novel statistical tolerance analysis method for assembled parts. Int J Prod Res 50(12):3498–3513
18. Khodaygan S, Movahhedy MR (2011) Tolerance analysis of assemblies with asymmetric tolerances by unified uncertainty–accumulation model based on fuzzy logic. Int J Adv Manuf Technol 53(5–8): 777–788
19. Whitney DE, Gilbert OL, Jastrzebski M (1994) Representation of geometric variation using matrix transforms for statistical tolerance analysis in assemblies. Res Eng Des 6:191–210
20. Ghie W, Laperrière L, Desrochers A (2010) Statistical tolerance analysis using the unified Jacobian–Torsor model. Int J Prod Res 48(15):4609–4630
21. Zhou S, Huang Q, Shi J (2003) State space modeling of dimensional variation propagation in multistage machining process using differential motion vectors. Robot Autom IEEE Trans 19(2):296–309